JOC*Article*

A Fast Radical Chain Mechanism in the Polyfluoroalkoxylation of Aromatics through NO_2 Group Displacement. Mechanistic and Theoretical Studies

Ismael Tejero, Imma Huertas, Àngels González-Lafont, José M. Lluch,* and Jordi Marquet*

Departament de Química, Universitat Autònoma de Barcelona, 08193 Bellaterra, Barcelona, Spain

lluch@klingon.uab.es; jordi.marquet@uab.es

Received September 16, 2004

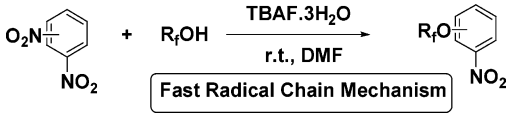

Introduction of polyfluoroalkoxy and polyfluoroalkylthio substituents in aromatic rings can be achieved with mild conditions and short times thorough reaction of concentrated solutions of dinitrobenzenes in DMF with polyfluoro alcohols and polyfluoro thiols in moderate excess, in the presence of excess tetrabutylammonium fluoride as a base. Mechanistic studies suggest that under these conditions a fast radical chain mechanism operates. This mechanism is elicited by oxidation of a Meisenheimer complex and proceeds through a radical aromatic substitution with the polyfluoroalkoxy or the polyfluoroalkylthio radicals as key intermediates. At low concentrations, entrainment can be achieved with superoxide anion. A rationale for this effect is discussed. Answers to particular questions about the proposed mechanism are achieved through a theoretical study at the B3LYP/6-31+G(d,p) level. Specifically, the competition between the radical mechanism and the corresponding polar one (classical S_NAr reaction) is studied in that way, with the conclusion that the key steps of the radical mechanism in our reaction conditions (polar aprotic solvent) are at least as efficient as the ones of the polar one, thus justifying the observed kinetic advantage for the chain reaction in the conditions where an efficient initiation occurs.

1. Introduction

Considerable time and attention have been and continue to be directed toward the synthesis of fluorinated organic materials.[1] Lately, in addition to the general interesting properties of these compounds, the demonstrated usefulness of biphasic fluorinated chemistry has added a more interest in their synthesis and the study of their properties.[2] Very recently, the combination of the advantages of palladium nanoparticles with their recovery in biphasic organic fluorous solvent systems has been reported.[3] In the case of polyfluoroalkoxyaromatics, two kinds of synthetic approaches have been described: (1) the reactions of electrophilic haloalkyl fluorides, fluoroalkenes, or fluoroalkylsulfonates with nucleophilic phenol derivatives[4,5] and (2) direct aromatic nucleophilic substitution reactions between polyfluoroalkoxide anions and chloro-, fluoro-, or nitro-substituted electron-poor aromatics in dipolar aprotic solvents, mainly HMPA.[5,6]

Even though nitro group displacement by trifluoroethoxide anion in HMPA is successful at room temperature with a variety of substituted nitrobenzenes, the reaction is slow, and rather high temperatures (150 °C) are needed for other polyfluoroalkoxydes, failing the reaction for branched ones such as hexafluoroisopropoxide anion.[6d]

The nucleophilic displacement of nitro groups in aromatic compounds constitutes a simple (in principle) but fascinating reaction with still many open questions. Despite the striking difference on nitrite leaving group ability in aliphatic or aromatic chemistry, it is generally

(1) *Organofluorine Chemistry. Principle and Commercial Applications*; Banks, R. E., Smart, B. E., Tatlow, J. C., Eds.; Plenum: New York, 1994.
(2) Horváth, I. T. *Acc. Chem. Res*. **1998**, *31*, 641 and references therein.
(3) Moreno-Mañas, M.; Pleixats, R. *Acc. Chem. Res*. **2003**, *36*, 638 and references therein.
(4) (a) Rico, I.; Wakselman, C. *Tetrahedron Lett*. **1981**, *22*, 323. (b) Rico, I.; Wakselman, C. *Tetrahedron* **1981**, *37*, 4209.
(5) Prescher, D.; Thiele, T.; Ruhmann, R. *J. Fluor. Chem*. **1996**, *92*, 1619.
(6) (a) Idoux, J. P.; Gupton, J. T.; McCurry, C. K.; Crews, A. D.; Jurss, C. D.; Colon, C.; Rampi, R. *J. Org. Chem*. **1983**, *48*, 3771. (b) Gupton, J. T.; Idoux, J. P.; DeCrescenzo, G.; Colon, C. *Synth. Commun*. **1984**, *14*, 621. (c) Gupton, J. T.; Hertel, G.; Decrescenzo, G.; Colon, C.; Baran, D.; Dukesherer, D.; Novik, S.; Liotta, D.; Idoux, J. P. *Can. J. Chem*. **1985**, *63*, 3037. (d) Idoux, J. P.; Madenwald, M. L.; Garcia, B. S.; Chen, D. L.; Gupton, J. T. *J. Org. Chem*. **1985**, *50*, 1876.

10.1021/jo048354m CCC: $30.25
Published on Web 02/02/2005

accepted that its nucleophilic displacement from electron-poor aromatics follows the polar S_NAr mechanism with the first step as the rate-limiting step, thus justifying the just commented difference in behavior.[7]

In many cases, typical S_NAr reactions show an unexpected dependence on conditions[8,9] and show radical trends,[10−12] radical anions have been detected,[13−17] oxygen has been shown to act as a promoter,[18] etc. All this behavior indicates a mechanistic complexity not yet resolved, since none of the mechanistic proposals advanced (generally including the radical anion as intermediate, i.e., the $S_{RN}2$ chain mechanism,[10,19,20] or electron transfer followed by collapse[21]) have resisted a close examination.[20,22−24] Among those S_NAr reactions with a peculiar behavior, the nucleophilic displacement of nitro group is central, with a significant number of examples described.[10,12,16,17,24]

We have been interested in the synthetic possibilities and the mechanistic ambiguities of the nucleophilic displacement of the nitro group in aromatics for some time,[24,25] and recently, we have described that anodic oxidation of the *σ*-complex intermediate in S_NAr reactions produces its instantaneous decomposition leading to substitution products.[25,26]

SCHEME 1

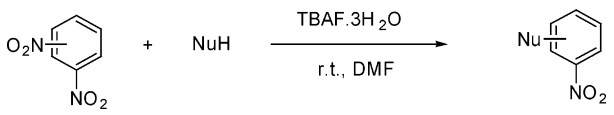

TABLE 1. Reactions of Dinitrobenzenes with Polyfluoro Alcohols and Polyfluorothiols in the Presence of TBAF·3H$_2$O in DMF[a]

entry	substrate	nucleophile	product	yield (%)	reaction time (h)
1	*p*-DNB	CF_3CH_2OH	**1a**	98	1
2	*p*-DNB	$(CF_3)_2CHOH$	**1b**[b]	30 (46)[c]	21
3	*p*-DNB	$CF_3(CF_2)_6CH_2OH$	**1c**	89	2
4	*p*-DNB	CF_3CH_2SH	**1d**	92	2
5	*o*-DNB	CF_3CH_2OH	**2a**	76 (86)[c]	1.5
6	*m*-DNB	CF_3CH_2OH	**3a**	70 (88)[c]	3
7	*m*-DNB	$CF_3(CF_2)_6CH_2OH$	**3c**	*d*	24
8	*m*-DNB	CF_3CH_2SH	**3d**	34 (83)[c]	5

[a] [DNB] = 0.02 M, [NuH] = 0.06 M, [TBAF·3H$_2$O] = 0.1 M. [b] In this reaction, a 11% yield of *p*-nitrophenol was obtained in addition to the substitution product. [c] The yield in parentheses is calculated with respect to the consumed (nonrecovered) starting material. [d] This product was not quantified since it was not possible to purify it.

In our experience, and from the results reported in the literature, the radical trends in S_NAr reactions are normally observed when working with an excess of nucleophile/base. In this work, we describe a synthetic improvement of the known reaction of polyfluoroalkoxylation by using an excess of nucleophile/base, a change that transforms the mechanism from a slow polar S_NAr to a very fast chain radical one. An experimental mechanistic study has been carried out, and the hypothesis advanced has been analyzed by theoretical methods. The polyfluoroalkoxylation reaction, being a relatively slow one, and the polyfluoroalkoxy anion and radical, being peculiar intermediates, allow us to observe clearly the change of mechanism, and the features of the radical one. The conclusions reached in this paper can probably apply to other S_NAr and related reactions that show narrow borderlines between polar and radical mechanisms, thus opening a via to improve our understanding of this borderline in reactions, such as S_NAr, that formally go through tetrahedral intermediates.

2. Experimental Results and Discussion

2.1. Preparative Reactions. Reactions of *m*-, *o*-, and *p*-dinitrobenzenes (DNB) with different polyfluoro alcohols or polyfluorothiols in the presence of tetrabutylammonium fluoride (TBAF) as base[28] are described in Scheme 1 and Table 1. A relatively concentrated solution of DNBs was used (0.02 M), nucleophiles and base were used in excess with respect to the substrate, and all the reactions were carried out at room temperature (the nature of the base has no influence in the reactions since similar results were achieved using sodium hydride). Reactions of *p*-DNB with 2,2,2-trifluoroethanol, 2,2,2-trifluoroethanethiol, and 1*H*,1*H*-pentadecafluoro-1-octanol are very fast and were completed in less than 2 h (entries 1, 3, and 4, Table 1). Reaction of *p*-DNB with a

(7) *Nucleophilic Aromatic Displacement. The Influence of the Nitro Group*; Terrier, F., Ed.; VCH: New York, 1991.
(8) (a) Shein, S. M.; Brykhovetskaya, L. V.; Pishchugin, F. V.; Starichenko, V. F.; Panfilov, V. N.; Voevodskii, V. V. *J. Struct. Chem*. **1970**, *11*, 228. (b) Blyumenfeld, L. A.; Brykhovetskaya, L. V.; Formin, G. V.; Shein, S. H. *Russ. J. Phys. Chem*. **1970**, *44*, 518.
(9) (a) Iwasaki, G.; Saeki, S.; Hamana, M. *Chem. Lett*. **1986**, 31. (b) Iwasaki, G.; Wada, K.; Saeki, S.; Hamana, M. *Heterocycles* **1984**, *22*, 1811.
(10) (a) Denney, D. B.; Denney, D. Z. *Tetrahedron* **1991**, *47*, 6577. (b) Denney, D. B.; Denney, D. Z.; Perez, A. J. *Tetrahedron* **1993**, *49*, 4463.
(11) Zhao, W.; Huang, Z. *J. Chem. Soc., Perkin Trans. 2* **1991**, 1967.
(12) Sammes, P. G.; Thetford, D.; Voyle, M. *J. Chem. Soc., Perkin Trans. 1* **1988**, 3229.
(13) (a) Bacaloglu, R.; Bunton, C. A.; Cericheli, G. *J. Am. Chem. Soc*. **1987**, *109*, 621. (b) Bacaloglu, R.; Bunton, C. A.; Cericheli, G.; Ortega, F. *J. Am. Chem. Soc*. **1988**, *110*, 3495. (c) Bacaloglu, R.; Bunton, C. A.; Ortega, F. *J. Am. Chem. Soc*. **1988**, *110*, 3503. (d) Bacaloglu, R.; Bunton, C. A.; Ortega, F. *J. Am. Chem. Soc*. **1988**, *110*, 3512.
(14) Bilkis, I. L.; Shein, S. M. *Tetrahedron* **1975**, *31*, 969.
(15) Relles, C. F.; Johnson, D. S.; Manello, J. S. *J. Am. Chem. Soc.* **1977**, *99*, 6677.
(16) (a) Abe, T.; Ikegami, Y. *Bull. Chem. Soc. Jpn*. **1976**, *49*, 3227. (b) Abe, T.; Ikegami, Y. *Bull. Chem. Soc. Jpn*. **1978**, *51*, 196.
(17) Sauer, A.; Wasgestian, F.; Barbasch, B. *J. Chem. Soc., Perkin Trans. 2* **1990**, 1317.
(18) Omelechko, E. N.; Ryabinin, V. A.; Shein, S. M. *Zh. Org. Khim*. **1982**, *18*, 1123.
(19) Marquet, J.; Jiang, Z.; Gallardo, I.; Batlle, A.; Cayón, E. *Tetrahedron Lett*. **1993**, *34*, 2801
(20) Galli, C.; Bunnett, J. F. *J. Am. Chem. Soc*. **1979**, *101*, 6137.
(21) (a) Zhang, X. M.; Yang, D. L.; Liu, Y. C. *J. Org. Chem*. **1993**, *58*, 224. (b) Zhang, X. M.; Yang, D. L.; Liu, Y. C. *J. Org. Chem*. **1993**, *58*, 7350.
(22) Makosza, M.; Podraza, R.; Kwast, A. *J. Org. Chem*. **1994**, *59*, 6796.
(23) Balslev, H.; Lund, H. *Tetrahedron* **1994**, *50*, 7899.
(24) (a) Mir, M.; Espin, M.; Marquet, J.; Gallardo, I.; Tomasi, C. *Tetrahedron Lett.* **1994**, *35*, 9055. (b) Marquet, J.; Casado, F.; Cervera, M.; Espin, M.; Gallardo, I.; Mir, M.; Niat, M. *Pure Appl. Chem*. **1995**, *67*, 703.
(25) Gallardo, I. Guirado, G.; Marquet, J. *J. Org. Chem*. **2002**, *67*, 2548.
(26) (a) Gallardo, I.; Guirado, G.; Marquet, J. *Chem. Eur. J*. **2001**, *7*, 1759. (b) Huertas, I.; Gallardo, I.; Marquet, J. *Tetrahedron Lett.* **2001**, *42*, 3439. (c) Gallardo, I.; Guirado, G.; Marquet, J. *Eur. J. Org. Chem*. **2002**, 251. (d) Gallardo, I.; Guirado, G.; Marquet, J. *Eur. J. Org. Chem*. **2002**, 261. (e) Gallardo, I.; Guirado, G.; Marquet, J. *J. Org. Chem*. **2003**, *68*, 631. (f) Gallardo, I.; Guirado, G.; Marquet, *J. Org. Chem*. **2003**, *68*, 7334.
(27) Schaal, R.; Peure, F. *Bull. Soc. Chim. Fr*. **1963**, 2638.
(28) Clark, J. H. *Chem. Rev*. **1980**, *80*, 429.

branched perfluoro alcohol such as 1,1,1,3,3,3-hexafluoro-2-propanol gave rise to the substitution product in fair yield, together with minor amounts of *p*-nitrophenol (entry 2, Table 1). Notice that, as far as we know, this is the first example of perfluoroalkoxylation using a α-branched nucleophile.

As expected, *m*-DNB was less reactive, but in any case good preparative yields were obtained with 2,2,2-trifluoroethanol and 2,2,2-trifluoroethanethiol (entries 6 and 8, Table 1). A similar result was obtained in the reaction of *o*-DNB and 2,2,2-trifluoroethanol (entry 5, Table 1).

The reaction of *m*-DNB with 1*H*,1*H*-pentadecafluoro-1-octanol produced the substitution product in fair yield (entry 7, Table 1); however, this reaction result could not be quantified due to the fact that the high viscosity of the product prevented any proper purification.

These preparative reactions, when compared with related ones reported in the literature,[6] show that the use of a relatively high concentration of aromatic substrate (0.02 M) and a modest excess of base and nucleophile accelerates significantly the processes, allowing the reaction to proceed under much milder conditions.

The nature of this faster process was first investigated by carrying out the reaction of *p*-DNB and 2,2,2-trifluoroethanol (entry 1, Table 1, 98% yield) in the presence of variable amounts of galvinoxyl as radical scavenger. Thus, in the presence of 0.3 equiv (molar ratio with respect to *m*-DNB) of galvinoxyl, only a 4% of substitution product was produced, and upon increasing the amount of galvinoxyl to 3.0 equiv, the reaction was stopped completely. Evidently this behavior, similar to other cases reported in the literature,[10−12] suggested the operation of a radical chain mechanism.

2.2. Mechanistic Studies. There are very few kinetic studies on nucleophilic aromatic substitutions with nitrite anion as a leaving group; however, some of them are interesting with respect to our own results. Thus, Schaal and Peure reported good first-order kinetics in the reaction of *p*-DNB with methoxide anion in methanol at concentrations lower than 1 M; however, at higher concentrations of nucleophile the rate constant increased exponentially.[27] Therefore, we decided to study the effect of substrate and base concentration on the evolution of our reactions. No good fit to standard kinetics was obtained under our conditions.

In Figure 1, the evolution of the absorbance at $\lambda = 302$ nm (absorption of the substitution product) with time in the reaction of *p*-DNB with 2,2,2-trifluoroethanol, at different starting substrate concentrations (keeping constant the molar relationship *p*-DNB/trifluoroethanol/TBAF, 1:5:5), is described. Surprisingly, a sharp change in behavior is observed when going from 3.0×10^{-4} to 4.0×10^{-4} M. In the first case, a relatively slow reaction evolution is observed, while upon a small increase in substrate concentration, the reaction becomes almost instantaneous.

In Figure 2, the evolution of the absorbance at $\lambda = 302$ nm with time in the reaction of *p*-DNB with 2,2,2-trifluoroethanol, at different base concentrations, using a concentration of substrate, *p*-DNB, 3.0×10^{-4} M (the fast reaction is not triggered in the conditions used in the experiments described in Figure 1), is described. Thus, when the molar relationship *p*-DNB/trifluoroethanol/FTBA is kept at 1:5:5, a relatively slow process is observed; however, when a relationship of 1:5:10 is used, the instantaneous process becomes apparent.

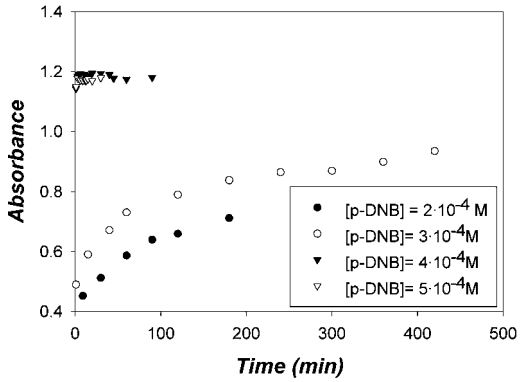

FIGURE 1. Evolution of absorbance ($\lambda = 302$ nm, product **1a**) vs time (min) in the reaction of *p*-DNB with 2,2,2-trifluoroethanol (molar ratio 5:1 with respect to *p*-DNB), in the presence of FTBA·3H_2O (molar ratio 5:1 with respect to *p*-DNB) in DMF, at different starting substrate concentrations.

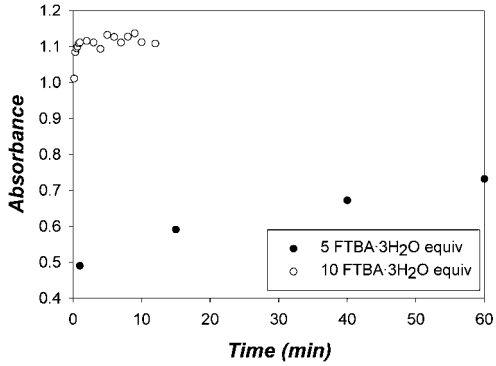

FIGURE 2. Evolution of absorbance ($\lambda = 302$ nm, product **1a**) vs time (min) in the reaction of *p*-DNB (starting concentration, 3.0×10^{-4}M) with 2,2,2-trifluoroethanol (molar ratio 5:1 with respect to *p*-DNB), in the presence of variable concentrations of FTBA·3H_2O (molar ratio 5:1, and 10:1, with respect to *p*-DNB) in DMF.

The obvious interpretation is the existence of a narrow mechanistic borderline between a slow mechanism and a fast, probably radical chain mechanism, considering the behavior of the preparative reaction in the presence of the radical scavenger galvinoxyl. This radical scavenger is not appropriate in reactions to be followed by UV/vis spectroscopy due to its strong absorption. Therefore, for qualitative kinetic analysis, sulfur was used. In Figure 3 the dependence of the "fast reaction" (5×10^{-4} M substrate concentration, in the conditions of Figure 1) on the presence of variable amounts of sulfur is described. Sulfur is not as strong as galvinoxyl as a radical scavenger; however, a significant retarding effect can be observed, even at molar relationships with respect to substrate, lower than one.

The existence of radical trends in the S_NAr reactions has been in many cases related with the hypothetic operation of the corresponding radical anions as intermediates. This is very well documented for $S_{RN}1$ reactions,[29] but no consistent confirmation of its general role has been found in the reactions of nitroaromatics despite a variety of proposals (see, for instance, refs 7, 8, 10, 13,

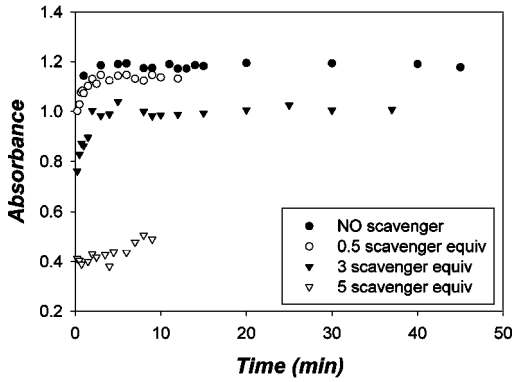

FIGURE 3. Evolution of absorbance (λ = 302 nm, product **1a**) vs time (min) in the reaction of *p*-DNB with 2,2,2-trifluoroethanol (molar ratio 5:1 with respect to *p*-DNB), in the presence of FTBA·$3H_2O$ (molar ratio 5:1 with respect to *p*-DNB) in DMF, with different amounts of added sulfur (radical scavenger).

16, 19, and 21). It is known that when a nitroaromatic compound is placed in front of high concentration of an anion, the corresponding radical anion can be detected by ESR spectroscopy.[17,30] This was also our case, since *p*-DNB in the presence of TBAF under our standard reaction conditions (1:5 molar relationship), in the absence of nucleophile, produced the *p*-DNB radical anion,[31] which could be detected by ESR. However, its presence does not necessarily mean its operation as intermediate. Indeed, the external electrogeneration of the radical anion produced an inhibition of the reaction when compared with a blank. The same happened when the generation of the radical anion was carried out photochemically with a reducing agent like triethylamine (Scheme 1). This behavior confirms similar results described in related systems.[23,24]

To propose a mechanistic hypothesis able to explain the experimental evidence, several points must be taken into account.

(a) Fluoride anion is a very hard anion, and its probability to participate in outer sphere electron-transfer processes must be negligible. On the other hand, it is a good nucleophile in polar aprotic solvents.[28]

(b) The double concentration effect, with respect to the substrate and with respect to the base, suggest a radical chain mechanism with an initiation step that is very dependent on both reagents.

(c) Scorrano's interpretation for the appearance of radical anions in the reaction mixtures of S_NAr processes of nitroaromatics includes a bimolecular oxidation of the Meisenheimer complex by its own starting nitroaromatic.[30] In our case, this could explain the observed concentration effects.

(d) Some of us have reported that stable Meisenheimer anion complexes, derived from nitroaromatic compounds, upon anodic oxidation undergo a fast decomposition, giving rise to substitution products. This decomposition takes place via elimination of a radical in the case of

SCHEME 2

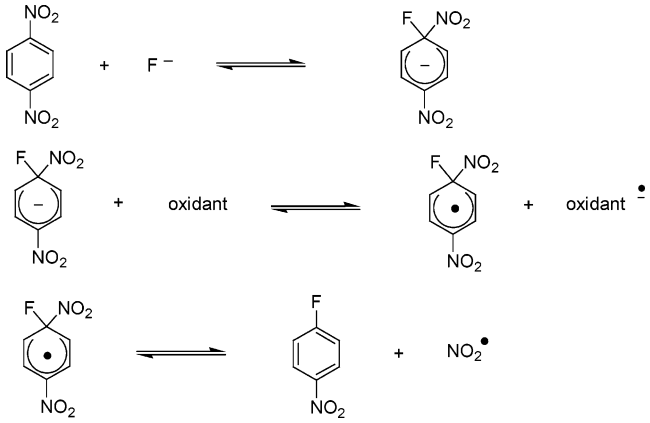

Meisenheimer complexes formed on a heteroatom-occupied position.[25,26]

(e) Even though in some particular cases nucleophilic substitution of aromatic halides[32] and other nonactivated aromatics[33] has been described to be elicited by oxidative catalysis, the well-established mechanism for those cases ($S_{ON}2$)[32] includes radical cations of the starting aromatic compound and of the final substitution product. Such intermediates have a very low probability to operate in our reactions since we are dealing with very electron-poor aromatics (nitroaromatic compounds).

(f) Even though direct oxidation of the nucleophile has been proposed as initiation step in some cases,[34] the observed concentration effects, the fact that fluoride anion is not basic enough to form discrete anions of the nucleophile, and the consideration of the redox potentials of the nucleophile anion and the electronically excited (under visible light) Meisenheimer complex make oxidation of the nucleophile in front of oxidation of a Meisenheimer complex a low probability initiation step in our standard reactions (however, see below the example of entrainment with superoxide anion).

In Scheme 2, a mechanistic hypothesis for the initiation steps of the mechanism is proposed. The Meisenheimer complex derived from *p*-DNB and fluoride anion would undergo oxidation by *p*-DNB,[30] and the fast evolution[25] of the resulting Meisenheimer radical would give rise to the nitrogen dioxide radical that would enter in the propagation steps of the mechanism. Even though the second step in Scheme 2 is probably endergonic, the fact that Meisenheimer complexes absorb strongly in the visible region (the reactions are carried out under ambient light) will make this electron-transfer step thermodynamically favorable. In addition, and in any case, an efficient radical chain may considerably amplify a weak initiation.[35]

In Scheme 3, the proposed propagation steps of the radical chain are described. Indeed, the mechanism

(29) (a) Bunnett, J. F. *Acc. Chem. Res*. **1978**, *11*, 413. (b) Savéant, J. M. *Tetrahedron* **1994**, *50*, 10117.
(30) Mariani, C.; Modena, G.; Pizzo, G. P.; Scorrano, G. *J. Chem. Soc., Perkin Trans. 2* **1979**, 1187.
(31) *High-Resolution ESR Spectroscopy*; Gerson, F., Ed.; Wiley: New York, 1970.
(32) (a) Alder, R. W. *J. Chem. Soc., Chem. Commun*. **1980**, 1184. (b) Eberson, L.; Jönsson, L. *J. Chem. Soc., Chem. Commun*. **1980**, 1187. (c) Eberson, L.; Jönsson, L. *J. Chem. Soc., Chem. Commun*. **1981**, 133. (d) Eberson, L.; Jönsson, L.; Wistrand, L. G. *Tetrahedron* **1982**, *38*, 1087. (e) Jönsson, L.; Wistrand, L. G. *J. Org. Chem*. **1984**, *49*, 3340.
(33) den Heijer, J.; Shadid, O. B.; Cornelisse, J.; Havinga, E. *Tetrahedron* **1977**, *33*, 779.
(34) Russell, G. A. *J. Am. Chem. Soc*. **1954**, *76*, 1595.
(35) Costentin, C.; Hapiot, P.; Médebielle, M.; Savéant, J. M. *J. Am. Chem. Soc*. **1999**, *121*, 4451.

SCHEME 3

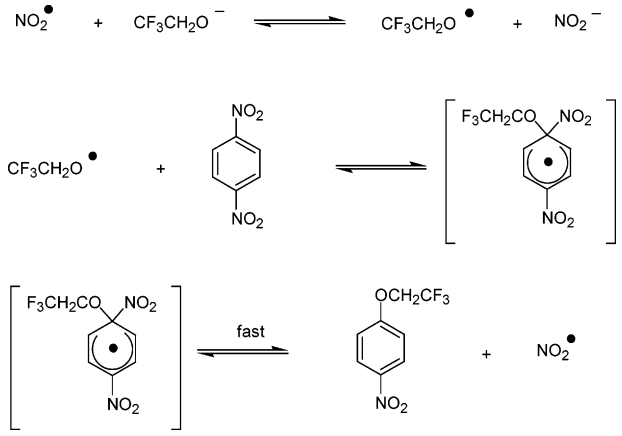

corresponds to a typical radical aromatic substitution,[36] although from the theoretical calculations described below it is not clear if the Meisenheimer radical operates as an intermediate or as a transition state. A downhill (see the Theoretical Calculations section) outer sphere electron transfer between an anion and a radical initiates the cycle.

It is known that superoxide anion is a good oxidant for relatively acidic protic substrates to the corresponding radical through a process that includes dismutation.[37,38] Therefore, trifluoroethanol radical could be generated alternatively by the action of superoxide anion on trifluoroethanol ($pK_a = 23.6$ in DMSO).[39] The fast reaction between *p*-DNB and trifluoroethanol could be elicited by addition of a catalytic amount of KO_2 (and an equimolecular amount of the 18-crown-6 ether to achieve its solubilization in DMF). This represents a good example of entrainment, and considering superoxide anion has no outher sphere electron-transfer oxidant properties,[37] this result strongly supports the operation of the trifluoroethoxy radical as intermediate.

Two questions appear when considering our mechanistic proposal:

(a) Can the radical aromatic substitution compete with the polar one?

(b) Is the step that opens the propagation cycle thermodynamically favorable?

Answers to these two questions have been obtained through theoretical calculations that are described in the following section.

3. Theoretical Calculations

The experimental results shown above indicate that *p*-DNB reacts with trifluoroethanol in the presence of base through a radical chain mechanism to give the corresponding aromatic substitution of the nitro group. Interestingly enough, related reactions of other alcohols do not seem to show radical behavior, and the well-known two-step polar S_NAr mechanism has been assigned.[7] To be able to discuss the feasibility of the different mechanisms through which these S_NAr reactions can take place, we have theoretically studied both the anionic and the radical addition−elimination mechanisms which are initiated by nucleophilic or radical attack at the π-aromatic molecule *p*-DNB of, respectively, the alkoxide anions or the alkoxy radicals derived from ethanol and 2,2,2-trifluoroethanol. In this section, we will first provide the computational details and then the theoretical results.

3.1. Computational Details. The quantum mechanical calculations have been carried out within the framework of the density functional theory (DFT),[40] which is reaching a widespread use in the calculation of quite sizable organic and inorganic molecules. The spin-unrestricted formalism has been used in solving the Kohn−Sham DFT equations.[41] The particular functional used has been the Becke three-parameter hybrid method using the Lee, Yang, and Parr correlation functional (B3LYP),[42] nowadays one of the most used functionals. The basis set chosen for the calculations had to be flexible enough to describe anionic species and, therefore, the split valence 6-31+G (d,p) basis set,[43] which includes d and p polarization functions on heavy and hydrogen atoms, respectively, and a diffuse sp shell on the heavy atoms, has been used. The diffuse functions provide ample space allowance for the additional electron in the anions. A preliminary Hartree−Fock study using the same basis set has also been carried out for the reactions of ethoxide anion and ethoxy radical.

Full geometry optimization and direct location of stationary points (minima and transition state structures) have been carried out by means of the Schlegel gradient optimization algorithm by using redundant internal coordinates.[44] Diagonalization of the potential energy analytical second-derivative matrix (Hessian) has been done to disclose the nature of the stationary point of the potential energy surface: no negative eigenvalues indicate a potential energy minimum, whereas one negative eigenvalue identifies a transition-state structure. In this second case, the eigenvector (transition vector) associated with the negative eigenvalue shows the direction along which the potential energy lowers. To ensure the connectivity between each transition state structure and the corresponding minimum energy points at both sides of it, the minimum energy path (MEP) has been calculated in each case by following the González−Schlegel mass-weighted internal-coordinates reaction-path algorithm.[45] Each MEP has been built up with a step size of 0.1 bohr $amu^{1/2}$.

The thermodynamic magnitudes have been computed by using the statistical thermodynamic formulation[46] of partition functions within the ideal gas, rigid rotor, and harmonic oscillator models. A pressure of 1 atm and a temperature of 298.15 K have been assumed in the calculations. The B3LYP analytical second derivatives of

(36) Tiecco, M. *Acc. Chem. Res.* **1980**, *13*, 51.
(37) Sawyer, D. T.; Valentine, J. S. *Acc. Chem. Res.* **1981**, *14*, 393.
(38) Nanni, E. J., Jr.; Stallings, M. D.; Sawyer, D. T. *J. Am. Chem. Soc.* **1980**, *102*, 4481.
(39) Bordwell, F. G. *Acc. Chem. Res.* **1988**, *21*, 456.
(40) Kohn, W.; Becke, A. D.; Parr, R. G. *J. Phys. Chem.* **1996**, *100*, 12974.
(41) (a) Honenberg, P.; Kohn, W. *Phys. Rev. B* **1964**, *136*, 864. (b) Kohn, W.; Sham, L. J. *Phys. Rev. A* **1965**, *140*, 1133.
(42) Becke, A. D. *J. Chem. Phys.* **1993**, *98*, 5648.
(43) *Ab Initio Molecular Orbital Theory*; Hehre, W. J., Radom, L., Schleyer, P. v. R., Pople, J. A., Eds.; Wiley: New York, 1986.
(44) Peng, C.; Ayala, P. Y.; Schlegel, H. B.; Frisch, M. J. *J. Comput. Chem.* **1996**, *17*, 49.
(45) Gonzalez, C.; Schlegel, H. B. *J. Phys. Chem.* **1990**, *94*, 5523.
(46) McQuarrie, D. A. *Statistical Thermodynamics*; University Science Books: Mill Valley, CA, 1973.

the potential energy with respect to the Cartesian coordinates have been used for the determination of vibrational frequencies. The imaginary frequency is neglected in the thermodynamic evaluation for transition-state structures.

The polarized continuum (overlapping spheres) model (PCM)[47] has been used to study the solvent effect for most of the reaction systems. Both electrostatic and nonelectrostatic terms have been included in the calculation. Acetonitrile ($\epsilon = 36.64$), a solvent of the list included in the Gaussian 98 package[48] whose dielectric constant value is very close to the DMF one, has been employed as solvent. As a matter of fact, several experiments were also done in acetonitrile, leading to results similar to the ones obtained using DMF as solvent. For the first propagation step of the radical chain, the self-consistent isodensity PCM (SCI-PCM)[49] model, whose solvent cavity is determined self-consistently from an isodensity surface, has been used.

The Gaussian 98 package[48] has been used to carry out all of the electronic calculations.

3.2. Theoretical Results. To begin, we will focus on the reaction of *p*-DNB with ethoxide anion and with ethoxy radical in gas phase. For the sake of comparison, we will show in parallel the results corresponding to the anionic and radical reactions. We have located 7 and 6 stationary points for the two processes at the Hartree−Fock electronic level, respectively, which leads to the potential energy profiles shown in Figure 4. From here on the subscripts A or R will mark the structures located along the anionic or the radical mechanisms, respectively. In the first case, the pathway evolves through an ion−molecule complex in the entrance channel (reactant complex, RC_A), a first transition-state structure ($TS1_A$), an intermediate (Int_A, which is a Meisenheimer σ-complex), a second transition- state structure ($TS2_A$), and an ion−molecule complex in the exit channel (product complex, PC_A), giving finally the final products (P_A, that is, *p*-ethoxynitrobenzene and nitrite anion). All these structures are much lower in potential energy than the reactants (R_A), as the global process is very exoergic. This is due to the fact that the net negative charge becomes more delocalized in going from reactants to products.

The sequence of stationary points along the radical pathway is analogous (but the reactant complex RC_R does not exist as a minimum), although the relative potential energies respect to *p*-DNB and ethoxy radical (R_R) are at least about 40 kcal/mol higher than the corresponding relative potential energies with respect to *p*-DNB and ethoxide anion along the anionic pathway. This is a consequence of the absence of a net negative charge that migrates during the process. Anyway, the global radical reaction turns out to be also exoergic leading to *p*-ethoxynitrobenzene and nitrite radical. Note that the neutral intermediate Int_R could be formally considered as an oxidated Meisenheimer complex (it has lost an electron). On the other hand, we have to point out that these Hartree−Fock calculations give a huge spin contamination of the radical species (expected values of within the range 1.2−1.5, instead of 0.75 which corresponds to a pure doublet) which indicates that a higher electronic level of calculation is strongly required for treating these processes in a suitable way.

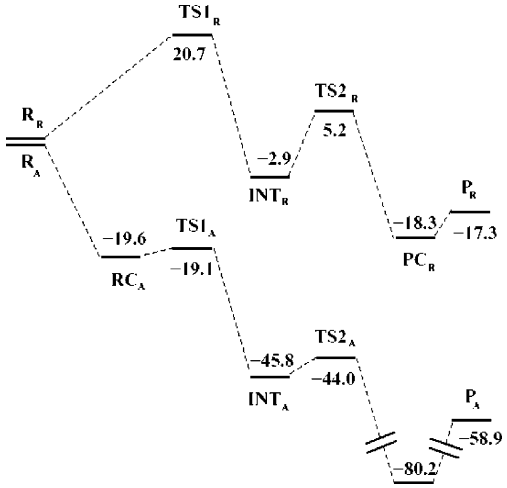

FIGURE 4. HF/6-31+G(d,p) gas-phase potential energy diagrams for the anionic (ethoxide anion) and radical (ethoxy radical) processes. Reactants R_A and R_R are taken as origin of energy for the anionic and the radical reactions, respectively. All values are given in kcal/mol.

The above-described Hartree−Fock picture clearly changes when electron correlation is introduced by means of B3LYP calculations (see Figure 5 for potential energies and Figures 6 and 7 for the geometries of the located stationary points).

As for the anionic mechanism, due to the lack of $TS2_A$, the Meisenheimer σ-complex is not longer a minimum. Then, only a transition-state structure (TS_A) has been located in a very flat region, with a geometry similar to the $TS1_A$ previously found at the Hartree−Fock electronic level. It has to be emphasized that correlation energy turns out to be essential in order to discuss the nature of the Meisenheimer complex. It is a shallow minimum at the Hartree−Fock electronic level, but it simply disappears as stationary point (neither an intermediate nor a transition-state structure) at the B3LYP electronic level. Likewise, the oxidated Meisenheimer complex is not a stationary point (due to the absence of $TS2_R$) for the B3LYP radical pathway too, for which only a transition-state structure (TS_R) appears after a reactant complex (RC_R) which did not exist at the Hartree−Fock electronic level. Analogously to the anionic case, the geometry of TS_R looks like that of $TS1_R$, but it is different from the geometry of the Int_R found at the Hartree−Fock electronic level.

From the energetic point of view, although the particular figures change, the anionic pathway is still

(47) (a) Miertus, S.; Scrocco, E.; Tomasi, J. *Chem. Phys.* **1981**, *55*, 117. (b) Miertus, S.; Tomasi, J. *Chem. Phys.* **1982**, *65*, 239.

(48) Frisch, M. J.; Trucks, G. W.; Schlegel, H. B.; Scuseria, G. E.; Robb, M. A.; Cheeseman, J. R.; Zakrzewski, V. G.; Montgomery, J. A., Jr.; Stratmann, R. E.; Burant, J. C.; Dapprich, S.; Millam, J. M.; Daniels, A. D.; Kudin, K. N.; Strain, M. C.; Farkas, O.; Tomasi, J.; Barone, V.; Cossi, M.; Cammi, R.; Mennucci, B.; Pomelli, C.; Adamo, C.; Clifford, S.; Ochterski, J.; Petersson, G. A.; Ayala, P. Y.; Cui, Q.; Morokuma, K.; Malick, D. K.; Rabuck, A. D.; Raghavachari, K.; Foresman, J. B.; Cioslowski, J.; Ortiz, J. V.; Stefanov, B. B.; Liu, G.; Liashenko, A.; Piskorz, P.; Komaromi, I.; Gomperts, R.; Martin, R. L.; Fox, D. J.; Keith, T.; Al-Laham, M. A.; Peng, C. Y.; Nanayakkara, A.; Gonzalez, C.; Challacombe, M.; Gill, P. M. W.; Johnson, B. G.; Chen, W.; Wong, M. W.; Andres, J. L.; Head-Gordon, M.; Replogle, E. S.; Pople, J. A. *Gaussian 98*, revision A.7−A.11; Gaussian, Inc.: Pittsburgh, PA, 1998.

(49) Foresman, J. B.; Keith, T. A.; Wiberg, K. B.; Snoonian, J.; Frisch, M. J. *J. Phys. Chem.* **1996**, *100*, 16098.

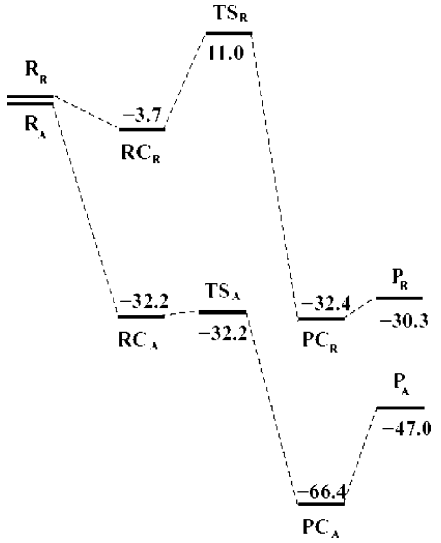

FIGURE 5. B3LYP/6-31+G(d,p) gas-phase potential energy diagrams for the anionic (ethoxide anion) and radical (ethoxy radical) processes. Reactants R_A and R_R are taken as origin of energy for the anionic and the radical reactions, respectively. All values are given in kcal/mol.

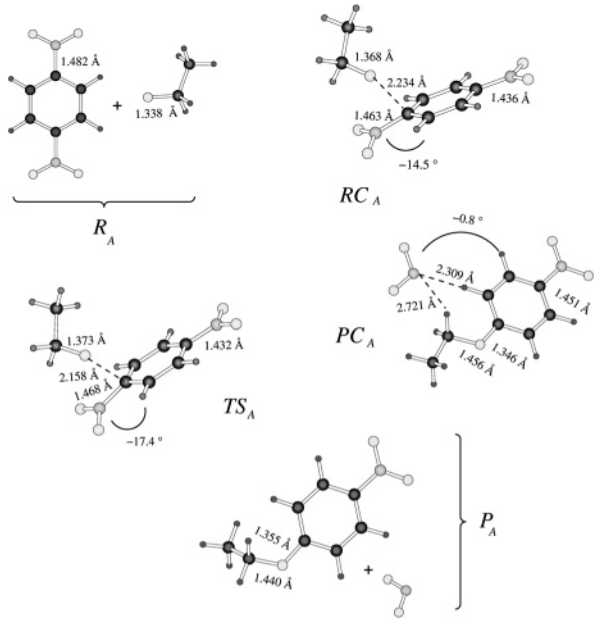

FIGURE 6. B3LYP/6-31+G(d,p) stationary point structures along the anionic (ethoxide anion) reaction path. All distance values given are in Å.

notoriously more favorable than the radical one in terms of relative potential energy at the B3LYP electronic level. In all cases the B3LYP spin contamination along the whole radical pathway was negligible ($\langle S^2 \rangle$ values never exceeded 0.751).

Until now we have only presented gas-phase calculations. To assess the solvent effect (acetonitrile), we have solvated the B3LYP gas-phase stationary points, their geometries being kept frozen. The new energy profiles are shown in Figure 8.

Solvation destabilizes clearly both the anionic and the radical pathways with respect to the corresponding reactants, although the two processes are still exergonic.

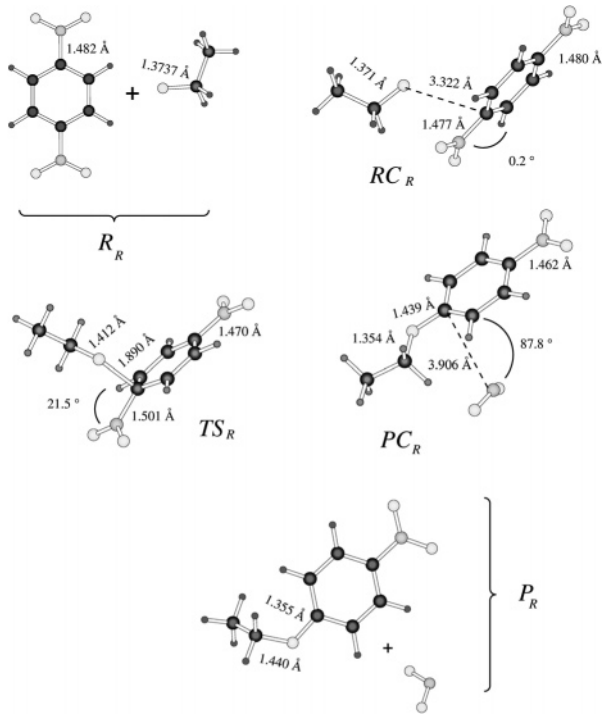

FIGURE 7. B3LYP/6-31+G(d,p) stationary-point structures along the radical (ethoxy radical) reaction path. All distance values given are in Å.

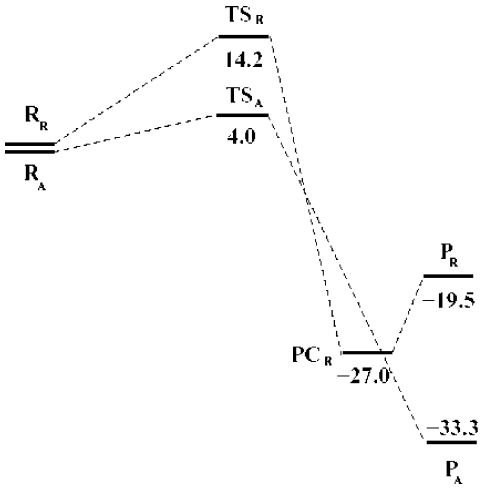

FIGURE 8. B3LYP/6-31+G(d,p)-solvated ($\epsilon = 36.64$) energy diagrams for the anionic (ethoxide anion) and radical (ethoxy radical) processes. Reactants R_A and R_R are taken as origin of energy for the anionic and the radical reactions, respectively. All values are given in kcal/mol.

The energies of the reactant complexes (RC_A and RC_R) become higher than their respective reactants (R_A and R_R), in such a way that they are no longer minima and they have not been represented in Figure 8. Likewise, the product complex PC_A goes above the product P_A and disappears as a minimum. The effect on the anionic pathway is quite dramatic as a consequence of the huge relative stabilization of the species in which the net negative charge is more localized, that is, nitrite anion on the product side and, especially, ethoxide anion in the reactant side. This anionic mechanism already involves a positive energy barrier, the energy difference between

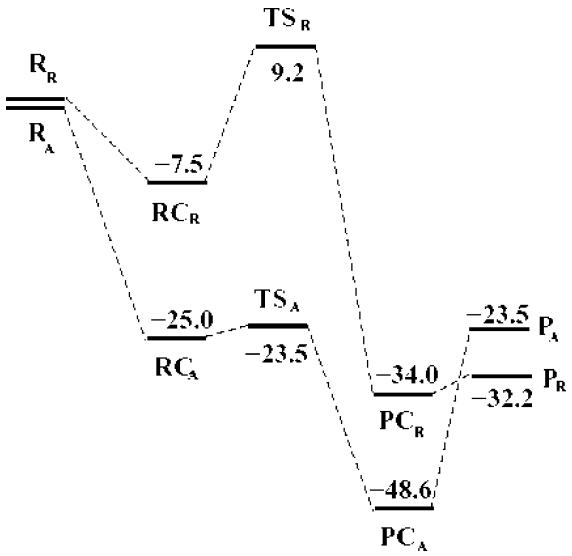

FIGURE 9. B3LYP/6-31+G(d,p) gas-phase potential energy diagrams for the anionic (2,2,2-trifluoroethoxide anion) and radical (2,2,2-trifluoroethoxy radical) processes. Reactants R_A and R_R are taken as origin of energy for the anionic and the radical reactions, respectively. All values are given in kcal/mol.

TS_R and TS_A having been reduced from 43.2 kcal/mol in gas phase to 10.2 kcal/mol in solution. As a result, the reaction of *p*-DNB with ethoxide anion is still predicted to be ostensibly faster than the reaction with ethoxy radical, although solvation with a polar solvent has reduced a lot the energy gap between them in comparison with the scenario in gas phase.

Let us turn our attention to the reaction of *p*-DNB with 2,2,2-trifluoroethoxide anion and with 2,2,2-trifluoroethoxy radical. Based on the above-described results, we have now directly used the B3LYP electronic level to study these reactions.

The corresponding gas-phase potential energy profiles and the geometries of the located stationary points are shown in Figures 9, 10, and 11, respectively. Comparing Figure 9 with Figure 5, it can be seen that the substitution of three hydrogen atoms by three fluorine atoms in the methyl group slightly stabilizes the radical mechanism, but it largely destabilizes the anionic pathway as a consequence of the electron-withdrawing power of those three fluorine atoms. As a result of that, the potential energy difference between TS_R and TS_A in the gas phase is now of only 32.7 kcal/mol, 10.5 kcal/mol lower than for the case of the derivatives of ethanol. In addition, an inversion in the energetic ordering of the final products occurs: P_A is 16.7 kcal/mol more stable than P_R for the case of ethanol, whereas it becomes 8.7 kcal/mol higher than P_R for the case of 2,2,2-trifluoroethanol.

The sequence and nature of the stationary points is the same as in the reactions with the derivatives of ethanol. Comparing geometries, TS_A for the reaction of 2,2,2-trifluoroethanolate anion (the distances for the O−C forming and the C−N breaking bonds are, respectively, 1.947 and 1.501 Å) appears to be somewhat displaced toward products relative to the same transition state structure for the reaction of ethanolate anion (the distances for the O−C forming and the C−N breaking bonds are, respectively, 2.158 Å and 1.468 Å). Conversely,

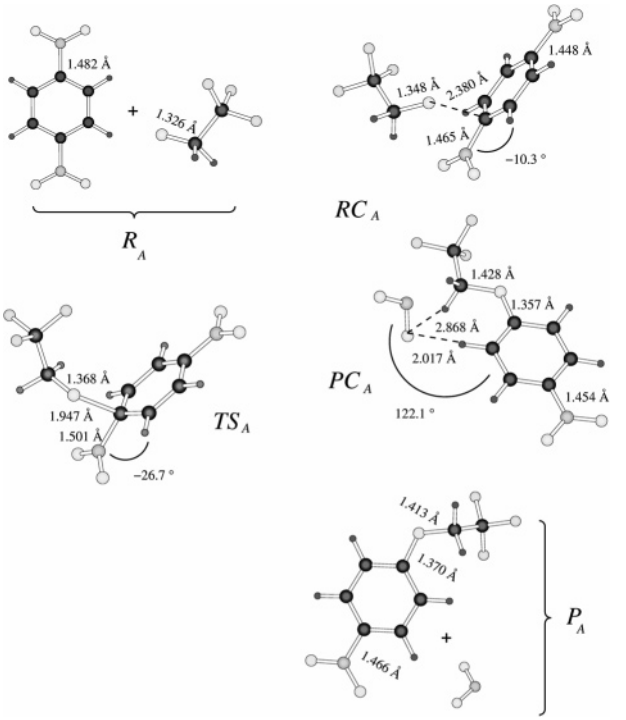

FIGURE 10. B3LYP/6-31+G(d,p) stationary-point structures along the anionic (2,2,2-trifluoroethoxide anion) reaction path. All distance values are given in Å.

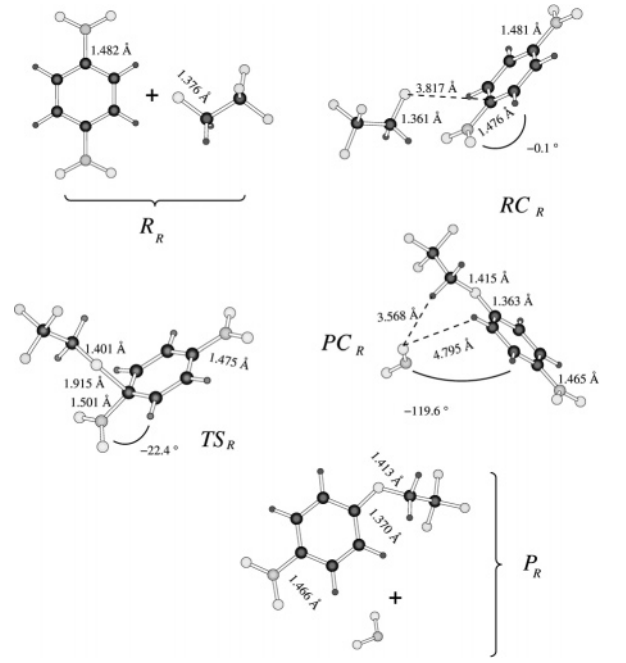

FIGURE 11. B3LYP/6-31+G(d,p) stationary-point structures along the radical (2,2,2-trifluoroethoxy radical) reaction path. All distance values are given in Å.

TS_R for the reaction of 2,2,2-trifluoroethoxy radical seems to be very slightly moved toward reactants respect to TS_R for the reaction of ethoxy radical. These facts are in agreement with the Hammond's postulate.

When the B3LYP gas-phase stationary points are solvated, the effects for the reactions with the derivatives of 2,2,2-trifluoroethanol (the energy profiles are pictured

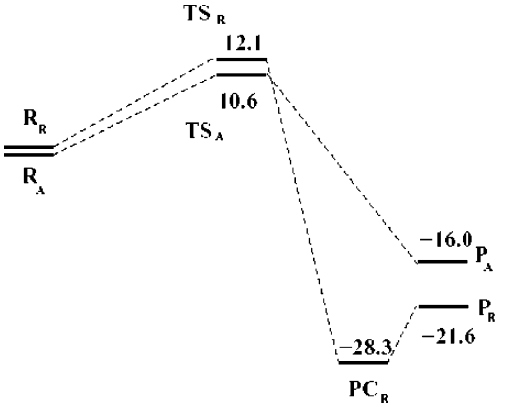

FIGURE 12. B3LYP/6-31+G(d,p)-solvated ($\epsilon = 36.64$) energy diagrams for the anionic (2,2,2-trifluoroethoxide anion) and radical (2,2,2-trifluoroethoxy radical) processes. Reactants R_A and R_R are taken as origin of energy for the anionic and the radical reactions, respectively. All values are given in kcal/mol.

in Figure 12) are quantitatively and qualitatively quite similar to the case of ethanol.

Due to solvation complexes RC_A, RC_R and PC_A disappear and both pathways are destabilized relative to the corresponding reactants, the effect on the anionic mechanism being again quite striking. This time the energy difference in the gas phase (32.7 kcal/mol) between TS_R and TS_A almost vanishes, becoming as small as 1.5 kcal/mol in acetonitrile as a solvent. Finally, we have calculated the zero-point energies, the thermal corrections, and the entropic contributions at the gas-phase stationary points in order to evaluate the Gibbs free energy barriers. When those three terms are added to the values given in Figure 12 we show that, in terms of free energy for the solvated reactions at 298.15 K, the anionic pathway is exergonic ($\Delta G° = -14.6$ kcal/mol) with a Gibbs free energy barrier of 23.8 kcal/mol, whereas the radical mechanism is also exergonic ($\Delta G° = -21.3$ kcal/mol) with a Gibbs free energy barrier of 23.6 kcal/mol. Very interestingly, we realize at this point that both barriers are equal in practice, although strictly speaking they have even reversed the ordering that had been found up to now in this paper.

We have also calculated the reaction energy of the formation of the 2,2,2-trifluoroethoxy radical according to the first propagation step of the radical chain (see Scheme 3). A B3LYP/6-31+G(d,p) calculation inside a solvent cavity (with full geometry optimization) leads to a reaction energy (without zero-point energy and thermal corrections) of −3.43 kcal/mol. This value confirms the feasibility of this propagation step as source of the 2,2,2-trifluoroethoxy radicals required to produce the radical substitution reaction.

Finally, it has to be noted that our B3LYP results predict that both the anionic and the radical pathways are concerted, with the bond formation and bond cleavage happening in the same step. So, the second and third propagation steps in Scheme 3 could be reduced to an unique step. In other words, it seems that, in this case, the reaction system crosses very fast through the region of the potential energy surface corresponding to the oxidated Meisenheimer structure, which is not a stable complex.

4. Conclusions

We have demonstrated that polyfluoroalkoxylation of aromatics can be carried out by mild substitution of a nitro group in nitroaromatic compounds in DMF, under conditions that include a relatively high concentration of substrate, nucleophile, and base. Mechanistic studies indicate the operation of a fast radical chain mechanism that includes an oxidation step; therefore, it seems we are in the presence of an example of reaction that is activated by oxidation ("one electron less").[50] Due to its biological relevance, the effect of superoxide anion as an activator is particularly significant.

The proposal for the propagation part of the mechanism has been studied by theoretical calculations, and the conclusion is that the radical substitution step is at least competitive with the corresponding reaction of the trifluoroethoxide anion. Therefore, it becomes evident that the chain mechanism can have a kinetic advantage once the proper initiation conditions are reached. The mechanism proposed, or a related one, can probably explain many experimental facts reported in the literature that suggest the existence of a radical mechanism in S_NAr reactions in certain conditions.

The theoretical study presented here is also a nice example of how the successive incorporation of different factors can even revert the conclusion first reached when using the lowest level of calculation, and conditions (gas phase), far away from the experimental reality (polar aprotic solvent).

5. Experimental Section

Commercial *o*-, *m*-, and *p*-dinitrobenzenes, 2,2,2-trifluoroethanol, 1,1,1,3,3,3-hexafluoro2-propanol, 1*H*,1*H*-pentadecafluoro-1-octanol, 2,2,2-trifluoroethanthiol, and tetrabutylammonium fluoride (as trihydrate, TBAF·$3H_2O$) were used without further purification.

General Procedure for the Reactions of Dinitrobenzenes with Polyfluoro Alcohols and Polyfluoro Thiols Described in Table 1. In a 100 mL round-bottomed flask with magnetic stirring was introducted 5.0 mmol of TBAF·$3H_2O$ in 45 mL of dry DMF. Then, 3.0 mmol of the nucleophile and 1.0 mmol of the DNB in 5 mL of dry DMF were added. The mixture was left under magnetic stirring for the time indicated in Table 1. Then, the reaction mixture was acidified with aqueous HCl and was extracted several times with ether. The organic layer was extracted again with aqueous HCl and dried and the solvent was evaporated, leaving the crude product that was purified from the remaining starting material (if any) and from the 4-nitrophenol (if any) by pressure column chromatography through silica gel using mixtures of hexane/ethyl acetate of increasing polarity as eluent.

***p*-(2,2,2-Trifluoroethoxy)nitrobenzene, 1a:** mp 75.5−76.5 °C (lit.[6a] mp 75−78 °C); ^{1}H NMR ($CDCl_3$) δ 4.43 (q, J = 8.0 Hz, 2H), 7.02 (d, J = 8.8 Hz, 2H), 8.23 (d, J = 8.8 Hz, 2H); MS *m/z* (relative intensity) 221 (M^+, 100), 191 (41), 156 (10), 111 (20), 92 (34), 83 (24), 64 (29).

***p*-(2,2,2-Trifluoro-1-trifluoromethylethoxy)nitrobenzene, 1b:** viscous oil; IR (KBr) 1594, 1525, 1494, 1350, 1257, 1200, 1175, 886, 800, 663 cm^{-1}; ^{1}H NMR ($CDCl_3$) δ 5.00 (septet, J = 2.7 Hz, 1H), 7.18 (d, J = 9.3 Hz, 2H), 8.26 (d, J = 9.3 Hz, 2H); ^{13}C NMR ($CDCl_3$) δ 74.6, 116.9, 120.7, 126.2, 144.3, 161.2. Anal. Calcd for $C_9H_5F_6NO_2$: C, 39.58; H, 1.85; N, 5.13. Found: C, 39.91; H, 1.98; N, 5.32.

(50) Chanon, M.; Rajzman, M.; Chanon, F. *Tetrahedron* **1990**, *46*, 6193.

***p*-(2,2,3,3,4,4,5,5,6,6,7,7,8,8,8-Pentadecafluorooctyloxy)-nitrobenzene, 1c:** mp 49.5−50.0 °C (lit.[51] mp 42−45 °C); ^{1}H NMR ($CDCl_3$) δ 4.55 (t, J = 12.4 Hz, 2H), 7.03 (d, J = 9.5 Hz, 2H), 8.23 (d, J = 9.5 Hz, 2H).

***p*-(2,2,2-Trifluoroethylthio)nitrobenzene, 1d:** viscous oil; IR (KBr) 1597, 1518, 1342, 1313, 1241, 1133, 1083, 845, 742, 639 cm^{-1}; ^{1}H NMR ($CDCl_3$) δ 3.58 (q, J = 9.5 Hz, 2H), 7.49 (d, J = 9.5 Hz, 2H), 8.16 (d, J = 9.5 Hz, 2H); ^{13}C NMR ($CDCl_3$) δ 37.7, 124.2, 124.9, 128.7, 143.1, 146.5. Anal. Calcd for $C_8H_6F_3NO_2S$: C, 40.51; H, 2.55; N, 5.91. Found: C, 40.89; H, 2.73; N, 6.15.

***o*-(2,2,2-Trifluoroethoxy)nitrobenzene, 2a.** This product was isolated by column chromatography as indicated in the "general procedure" and purified by distillation (114 °C, 3 Torr):[6a] ^{1}H NMR ($CDCl_3$) δ 4.47 (q, J = 8.0 Hz, 2H), 7.14 (m, 2H), 7.57 (dt, J = 7.3, 2.2 Hz, 1H), 7.85 (dd, J = 8.0, 2.2 Hz, 1H).

***m*-(2,2,2-Trifluoroethoxy)nitrobenzene, 3a:** mp 58.0−58.5 °C (lit.[6a] mp 57−59 °C); ^{1}H NMR ($CDCl_3$) δ 4.43 (q, J = 8.0 Hz, 2H), 7.29 (dd, J = 8.0 Hz, J = 2.2 Hz, 1H), 7.49 (t, J = 8.0 Hz, 1H), 7.77 (t, J = 2.2 Hz, 1H), 7.93 (dd, J = 8.0 Hz, J = 2.2 Hz, 1H); MS *m/z* (relative intensity) 221 (M^+, 100), 175 (32), 111 (31), 92 (35), 83 (16).

***m*-(2,2,3,3,4,4,5,5,6,6,7,7,8,8,8-Pentadecafluorooctyl-oxy)nitrobenzene, 3c:** viscous oil that could not be purified (the structure assignation must be considered as tentative); ^{1}H NMR ($CDCl_3$) δ 4.54 (t, J = 12.5 Hz, 2H), 7.29 (ddd, J = 1.0, 2.5, 8.4 Hz, 1H), 7.50 (dd, J = 8.0, 8.4 Hz, 1H), 7.78 (dd, J = 2.0, 2.5 Hz, 1H), 7.93 (ddd, J = 1.0, 2.0, 2.0, 1H); MS *m/z* (relative intensity) 521 (M^+, 100).

***m*-(2,2,2-Trifluoroethylthio)nitrobenzene, 3d:** viscous oil; IR (KBr) 1528, 1350, 1264, 1241, 1125, 1081, 802, 731 cm^{-1}; ^{1}H NMR ($CDCl_3$) δ 3.52 (q, J = 9.4 Hz, 2H), 7.51 (t, J = 7.8 Hz, 1H), 7.76 (m, 1H), 8.13 (m, 1H), 8.30 (t, J = 1.8 Hz, 1H); ^{13}C NMR ($CDCl_3$) δ 37.3, 122.6, 124.2, 125.0, 125.4, 130.05, 136.2, 136.6. Anal. Calcd for $C_8H_6F_3NO_2S$: C, 40.51; H, 2.55; N, 5.91. Found: C, 40.37; H, 2.66; N, 5.68.

Acknowledgment. We are grateful for financial support from the Spanish "Ministerio de Ciencia y Tecnología" and the "Fondo Europeo de Desarrollo Regional" through Project Nos. BQU2002-00301 and BQU2003-05457 and from the "Generalitat de Catalunya" through Project No. 2001SGR 00180. Likewise, we acknowledge the use of the computational facilities of the CESCA.

Supporting Information Available: Tables 1−36 show the geometries, energies, and number of imaginary vibrational frequencies of the stationary points located. This material is available free of charge via the Internet at http://pubs.acs.org.

JO048354M

(51) Prescher, D.; Thiele, T.; Ruhmann, R. *J. Fluorine Chem*. **1996**, *79*, 145.